GEOCRITICAL RESERVOIR FLOW SIMULATION AND DISPLAY USING OPEN POROUS MEDIUM (OPM) CODE

J Rugis[1], P Leary[1], P Malin[1] and J Pogacnik[1]

[1]Institute of Earth Science & Engineering, University of Auckland, New Zealand

j.rugis@auckland.ac.nz

Keywords: *Simulation, reservoir flow, open-source, lognormal*

ABSTRACT

Spatial fluctuations for *in situ* flow structures tend to be spatially highly erratic and to scale with physical dimension. Such reservoir flow spatial fluctuation properties are reflected in the lognormal distributions of well productivities in some oil/gas and geothermal fields. Ability to efficiently recognize and manage large-scale spatially erratic flow structures when they are present is thus key to cost-effective reservoir operation.

The Open Porous Medium (OPM) consortium provides industry-compatible open-source finite-element flow simulation code with robust handling of spatially complex flow distributions. For situations where the flow is dominated by fractures, 3 empirical rules be stated: (i) power-law-scaling fracture density fluctuations exist over cm-km scale lengths; (ii) changes in permeability $\delta\kappa$ are proportional to the product of permeability κ and changes in porosity $\delta\varphi$, $\delta\kappa \propto \kappa\, \delta\varphi$; and (iii) κ is lognormally distributed, $\kappa \propto \exp(\alpha\varphi)$, $\alpha >> 1$. OPM can be adapted to systematic modelling of this type of heterogeneity, which we show can be detected by new methods in seismic emission tomography.

We exhibit here the aptitude of OPM code for simulating and displaying spatially complex, single-phase flow distributions. We show that it can be efficient and accurate used for modeling of reservoir where significant flow heterogeneity is responsible for lognormal distributions of well productivity.

1. GEOCRITICALITY: THE THREE RULES

Out of computational necessity some past geothermal reservoir observations and concepts have been fit to earth models comprising a small range of geologically identified formations (e.g., Grindley 1965 MDW 1977; DSIR 1981; Wood 1992; Allis 2000; White et al 2005; Bignal & Milicich 2012). These formations are generally assumed to have essentially uniform physical properties (e.g., Theis 1935, 1952; Biot, 1941; Horner 1951; Freeze 1975; Earlougher 1977; Kitanidis 1990; Horne 1995; Mannington et al 2004; Ingebritsen et al 2010; Gudmundsdottir 2012; Ricard et al 2012). In some cases non-uniformity in physical properties has been limited to adding various mechanically discontinuous fault structures as needed to adjust flow models to observed pressure and flow data.

In situations where reservoir properties are highly heterogeneous, the limitations of such reservoir modeling assumptions have long been recognised (Warren & Skiba 1964; Freeze 1975; Smith & Freeze 1979; Dagan 1981, 1982; Desbarats 1987; Kitanidis 1990). For example, because of pervious computational limitations, it has been practically difficult to use them to forecast new well productivity, along with well-core permeability, and trace element and ore grade distributions. In many instances these properties are found to follow lognormal distributions (Law 1944; Warren & Skiba 1964; Jensen, Hinkley & Lake 1987; Limpert, Stahel & Abbt, 2001; Leary & Al Kindy 2002; US Energy Information Administration 2011; Grant 2009; Leary, Pogacnik & Malin 2012; Leary et al 2013a,c). One modeling approach for dealing with these observations is to include multiple layers with multiple properties, the net distribution of which approach lognormality (M. O'Sullivan, personal communication, 2013). Quantitatively, such distributions imply at there exists large scale features that span the sample volume (e.g. Mitzenmacher, 2004), thereby helping account for many of the observed features of the flow field.

To understand the effects of introducing more and more heterogeneity into a flow model consider first a simple system of geologically-recognized layers. If we log a well drilled through a reservoir model composed of a few laterally uniform layers, we record a series of step-functions in logged properties at their boundaries. As discussed in Appendix A, the Fourier spectrum of such a numerical log has a specific property explicitly associated with step functions:

$$S(k) \sim 1/k^2, \qquad (1a)$$

where k is spatial frequency and $S(k)$ the property spatial variation power at spatial frequency k. Along layers $S(k)$ would remain constant until a lateral boundary, such as a fault or significant facies change is encountered. The latter boundaries would introduce 2D and 3D forms of Eq. 1a. More complex models can thus be approached by increasing the number of blocks.

In this paper we present an alternative approach to highly heterogeneous reservoirs, one based on the spectral characteristics of well logs, cores, and new seismic emission tomography results (Geiser et al., 2011). The approach can include formation boundaries, faults, and facies changes.

Our development begins with noting that in highly heterogeneous rocks, well logs along *any* direction in geologically recognized layers show spectral distributions different from Eq.1a. In these cases properties scale inversely with the first rather than the second power of spatial frequency,

$$S(k) \sim 1/k^1, \qquad (1b)$$

where the range of observed spatial frequencies extends over five decades, ~1/km < k < ~1/cm (Leary 1991, 1997, 2002; Bean 1996; Shiomi, Sato & Ohtake 1997; Dolan, Bean & Riollet 1998; Marsan & Bean 1999; Leary et al 2013b,c).

We note in passing that well-log power law scaling power spectrum (1b) is also distinct from the spectrum of 'white' or 'Gaussian' spatial fluctuations characterized by

$$S(k) \sim 1/k^0 \sim const. \quad (1c)$$

In Appendix A we shows how physical structures characterized by spatial fluctuations associated with the spectra in Eq.s 1 appear in map view. These maps illustrate how the physical structure of crustal rock characterized by spectrum (1b), is not effectively approximated by blocked or uniformly random properties. As a result, geophysical processes in highly heterogeneous rocks characterised by well-log spectra (1b) need visualisation and conceptual modelling tools that do not depend on quasi-uniformity and/or spatial averages.

Paralleling well-log spectral systematics (1a)-(1c) discussed in Appendix A, Appendix B reviews well-core spatial fluctuation data that reveal a systematic *in situ* link between porosity and permeability. The examples given in Appendix B show that logarithm of permeability fluctation is more closely related to the distribution of porosity fluctuations than permeability fluctuations themselves.

For modeling purposes, well-core fluctuation systematics thus suggest two expressions relating *in situ* permeability to *in situ* porosity. At the tenths of metres to metres scale, spatial fluctuations in porosity $\delta\varphi$ closely track spatial fluctuations in the logarithm of permeability $\delta\log\kappa$,

$$\delta\varphi \sim \delta\log\kappa. \quad (2)$$

At the integrated tens to hundreds of metres scale of spatial fluctuations (2), a large-scale porosity-permeability relation emerges as the lognormal distribution,

$$\kappa \propto exp(\alpha\varphi), \quad (3)$$

in which the degree of lognormality is controlled by the empirical parameter α (Leary et al 2012).

Empirical conditions (1b), (2) and (3) provide a physical basis for *in situ* flow modeling in highly heterogeneous reservoirs (Leary et al 2013a). This approach gives a physical basis to the statistical properties of reservoir heterogeneity observed by Warren & Skiba (1964), Freeze (1975), Smith & Freeze (1979), Dagan (1981, 1982), Desbarats (1987) and Kitanidis (1990). We term the new modeling approach 'geocriticality' because the physical processes underlying (1b), (2) and (3) are closely related to 'critical' phenomena observed for a range of physical systems (Leary 1997, 2002).

Our intent here is to introduce the OPM computational environment in which to implement the geocritical reservoir model in the context of advanced oil and gas reservoir flow modeling. We display field and OPM-generated synthetic geophysical data related to *in situ* fracture distributions -- that is, consistent with spatial fluctuations with spatial frequency spectrum (1b) and lognormal permeability distributions (3) -- using software tools designed for modelling and for visual inspection of complex 3D spatial arrays.

2. OPEN POROUS MEDIA INITIATIVE

The Open Porous Media (OPM) initiative was launched in June 2009 at Statoil Research Center in Norway, and is currently supported by six research groups and several industry partners both in Norway and Germany[1]. The primary result of the initiative has been the development of an open-source simulator suite for flow and transport in porous media. The entire software suite has been made available under the terms of the GNU General Public License (GPL) version 3.

The development of new POM simulation codes is funded in part by industry (Statoil and Total) and by public grants from the Research Council of Norway. Current officially funded OPM development is focused on oil reservoir engineering, enhanced oil recovery and CO2 sequestration (Lie 2012, Lie 2013). However, contributions aimed at different fields are encouraged.

All of the OPM source code is hosted in GitHub public repositories[2]. User contributions follow the "fork and pull" model in which contributors create their own fork of the common repository, make changes, and then notify the maintainers who pull the changes back into the common repository.

2.1 OPM modifications

OPM is itself an extension module to the Distributed Unified Numerics Environment (DUNE), a software toolbox for solving partial differential equations using grid based methods[3]. OPM executable code can be built either as a DUNE module, using the standard dune control mechanism, or in stand-alone mode using cmake.

Both OPM and DUNE are written in the C++ language and make use of an object oriented programming style. The extensive OPM application programming interface (API) documentation takes the form of formatted HTML pages suitable for viewing in a web browser.

One of the primary advantages of open-source code is, of course, the ability to modify its functionality. In the work presented in this paper, we have employed the incompressible two-point-flux-approximation (TPFA) fluid pressure solver (Ponting 1992) class Opm::IncompTpfa. As given in its original form, this class only accepts bulk values for porosity and permeability from the properties class Opm::IncompPropertiesBasic. We have added public member functions setPorosity and setPermeability to the IncompPropertiesBasic class to accept arbitrary porosity and permeability fields.

OPM includes the class Opm::writeVtkData for writing out simulation results to a file suitable for visualisation in ParaView[4]. For completeness, we have modified this class so that the output file includes the 3D porosity and permeability fields as well as the computed pressure and velocity fields.

[1] http://www.opm-project.org

[2] github.com

[3] http://www.dune-project.org

[4] http://www.paraview.org

3. PROCESSING WORKFLOW

Our geocritical reservoir modelling workflow begins with the generation of synthetic 3D porosity and permeability blocks consistent with the rules given in Section 1. We explore the implications of varying alpha in equation (4) through values of 3, 10, 20 and 30.

We submit the porosity/permeability blocks to our modified OPM simulation code for determination of pressure and velocity.

Finally, we use ParaView to visually explore the simulation results.

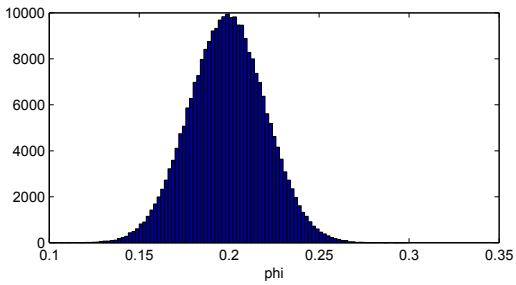

Figure 1: Porosity histogram.

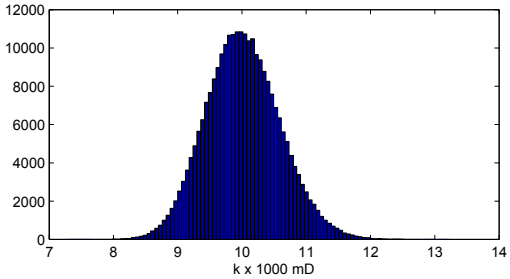

Figure 2: Permeability histogram – alpha 3.

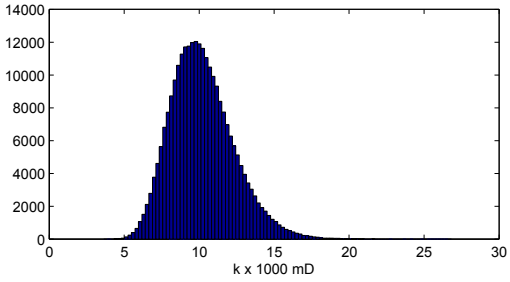

Figure 3: Permeability histogram – alpha 10.

3.1 Synthetic data generation

In this paper, using MatLab, we started with the creation of a spatially filtered 64x64x64 porosity structure (2) having a filter exponent of 1.35. As shown in Figure 1, this porosity structure has an overall normal (Gaussian) population distribution.

Again using MatLab, we created permeability structures according to equation (4) over a range of four different values for alpha. Figures 2-5 show resultant permeability population histograms for alpha equal to 3, 10, 20 and 30.

Observe that the permeability population distribution starts out as normal with alpha equal to 3, then becomes increasing lognormal as alpha is increased.

We saved each 64x64x64 porosity/permeability pair out to a MatLab data file.

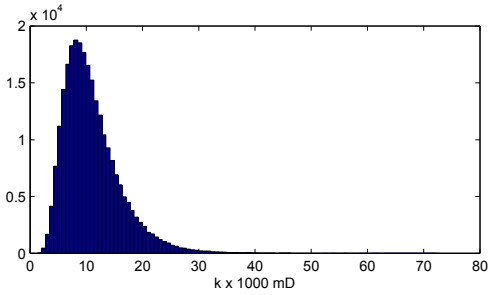

Figure 4: Permeability histogram – alpha 20.

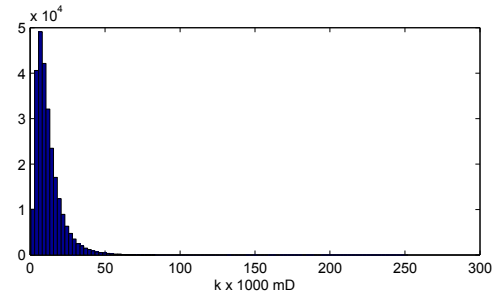

Figure 5: Permeability histogram – alpha 30.

3.2 Simulation

We wrote a C++ wrapper program to read Matlab data files, call our modified OPM modules, run an OPM 64x64x64 3D simulation and output ParaView compatible result files for visualisation.

Note that OPM has inbuilt support for explicit physical units of measurement, with the International System of Units as default. As an example, the commonly used unit of measurement for permeability, milli-Darcy, is internally translated to its correct value in metres squared.

For this simulation the grid units were left as the default, which gave an overall physical model space cube of 64 metres per side. We chose a somewhat modest inflow/outflow rate of 10 litres per second with injection/extraction points centered on opposite faces, 6 metres in from the outside.

The OPM simulator was run for each of the four alpha values. Central slices of the resultant velocity field are shown in Figures 6-9. The injection/extraction points are clearly visible. Velocity magnitudes range from very nearly zero to approximately 1 mm/sec. For these models, the maximum differential pressure (not illustrated) ranges from approximately 550 to 890 kPa.

We see that, as alpha increases, velocity filaments begin to form. These velocity filaments are suggestive of flow pathways which are explored further in the next section.

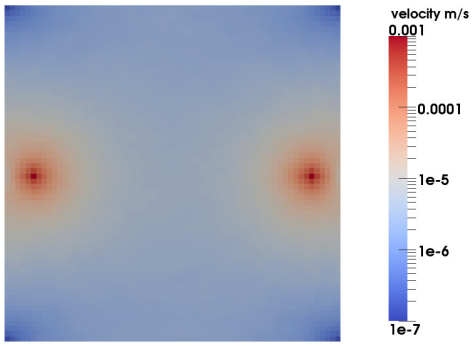

Figure 6: Velocity slice – alpha 3.

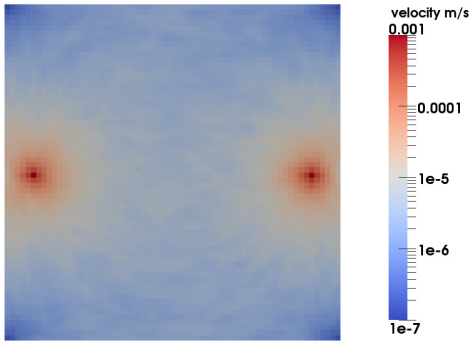

Figure 7: Velocity slice – alpha 10.

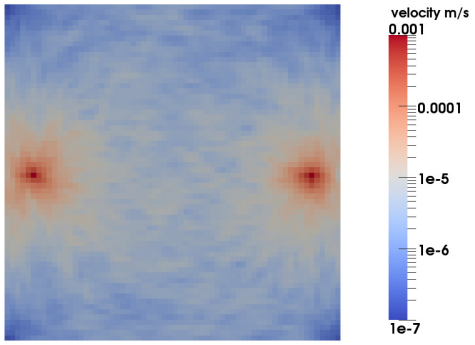

Figure 8: Velocity slice – alpha 20.

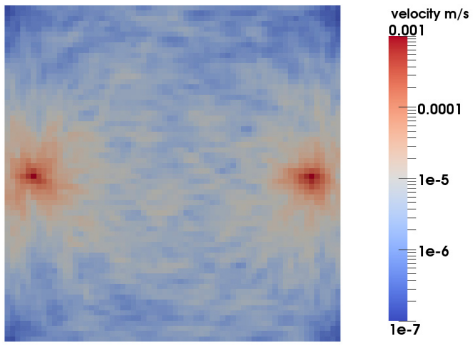

Figure 9: Velocity slice – alpha 30.

3.3 Additional 3D visualisation

Paraview software includes a collection of additional processing "filters" that target advanced visualisation. One of the filters can be used to create flow streamlines from seed particles placed in the velocity field.

Streamlines are shown for the four alpha values in Figures 10-13. We can see that, consistent with the notion of geocriticality, the particle flow streamlines become increasingly perturbed as alpha is increased.

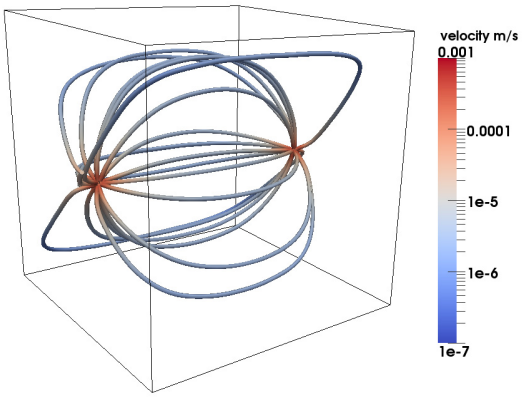

Figure 1: Streamlines – alpha 3.

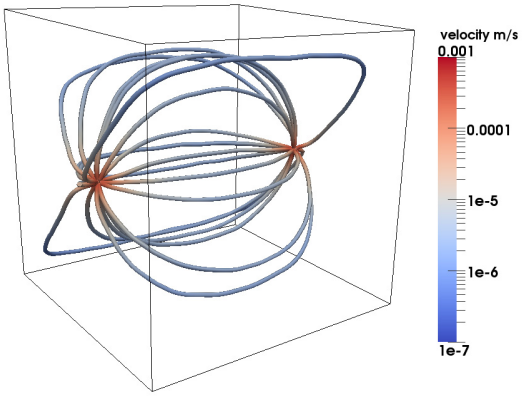

Figure 2: Streamlines - alpha 10.

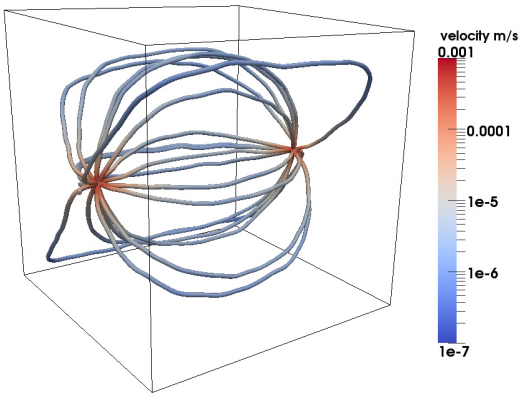

Figure 3: Streamlines - alpha 20.

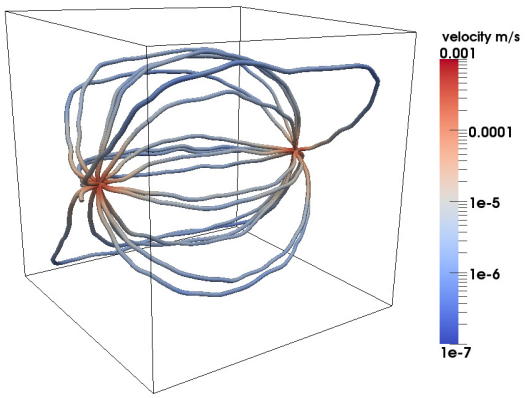

Figure 4: Streamlines - alpha 30.

3. CONCLUSION

We have successfully enhanced the Open Porous Media software tool suite to accommodate heterogeneous porosity and permeability structures that are consistent with our theory of geocriticality. We have also used visual streamlines to indicate the perturbed particle pathways associated with an increased permeability factor. These steps are part of a sequence of OPM developments designed to accommodate the modelling of large-scale active-reservoir surface seismic monitoring data arising from reservoir fluid pressurisation events (Leary et al 2013a).

ACKNOWLEDGEMENTS

The authors would like to thank the Open Porous Media initiative contributors for making their software available as open-source. We also acknowledge all of the sponsors and contributors to the ParaView open-source visualisation software package.

REFERENCES

Allis, RC & Zhan, XY, 2000, Predicting subsidence at Wairakei and Ohaaki geothermal fields, New Zealand, Geothermics 29, 479-497.

Bean C. J., 1996, Geophys. Res. Lett., 23, 3119-3122.

Bean, C. J., 1996, On the cause of 1/f-power spectral scaling in borehole sonic logs, Geophys. Res. Lett. 23:3119-3122.

Bignal G & Milicich SD (2012) Kawerau Geothermal Field: Geological Framework, GNS Science Report 2012/33, pp36.

Biot MA (1941) General theory of three-dimensional consolidation, Journal of Applied Physics 12, No. 2, 155-164.

Bracewell, R.N., The Fourier Transform and Its Applications (McGraw-Hill, 1965, 2nd ed. 1978, revised 1986).

Dagan G, 1981, Analysis of flow through heterogeneous random aquifers by the method of embedding matrix, I, Steady flow, Water Resources Research 17, 107-121.

Dagan G, 1982, Analysis of flow through heterogeneous random aquifers, I, Unsteady flow in confined formations, Water Resources Research 18, 1571-585.

Desbarats, AJ, 1987, Numerical estimation of effective permeability in sand-shale formations, Water Resources Research 23, 273-286.

Dolan, S. S., Bean, C. J., and Riollet B., 1998, The broadband fractal nature of heterogeneity in the upper crust from petrophysical logs, Geophys. J. Int. 132:489-507.

DSIR Geothermal Report 7 (1981) The Ngawha Geothermal Area, New Zealand Department of Scientific and Industrial Research, ISSN 0110-7259/ISBN 0-477-06689-5, pp167.

Earlougher R.C. (1977) Advances in Well Test Analysis, Society of Petroleum Engineers, Dallas, pp264.

Freeze, R. A. (1975), A Stochastic-Conceptual Analysis of One-dimensional Groundwater Flow in Non-uniform Homogeneous Media, Water Resources Research, 11, 725-741.

Grant MA (2009) Optimization of drilling acceptance criteria, Geothermics 38, 247–253.

Grindley, G. W., 1965, The geology, structure and exploitation of the Wairakei geothermal field, GrantTaupo, New Zealand: N.Z. Geological Survey Bulletin 75, 131.

Gudmundsdottir H (2012) A coupled wellbore-reservoir simulator utilising measured wellhead conditions, MS Thesis, School of Engineering and Natural Science, University of Iceland.

Horne RN, 1995, Modern Well Test Analysis, Petroway Inc, ISBN 0-9626992-1-7, pp257.

Horner, DR, 1951, Pressure build-up in wells, In: Third World Petroleum Congress, The Hague, pp 503-523; also Pressure Analysis Methods, SPE Preprint Series 9, pp 25-43, 1967.

Ingebritsen SE, Geiger S, Hurwitz S & Driesner T (2010) Numerical simulation of magmatic hydrothermal systems, Reviews of Geophysics 48, 1-33.

Jensen JL, Hinkley DV & Lake LW (1987) A statistical study of reservoir permeability: distributions, correlations, and averages, SPE Formation Evaluation, December 1987.

Kitanidis PK, 1990, Effective hydraulic conductivity for gradually varying flow, Water Resources Research 26, pp 1197-1208.

Law J (1944) A statistical approach to the interstitial heterogeneity of sand reservoirs, Technical Publication 1732, Petroleum Technology 7, May 1944.

Leary PC (1991) Deep borehole log evidence for fractal distribution of fractures in crystalline rock. Geophysical Journal International 107, 615-628.

Leary PC (1997) Rock as a critical-point system and the inherent implausibility of reliable earthquake prediction, Geophysical Journal International 131, 451-466.

Leary P.C. & F. Al-Kindy, 2002. Power-law scaling of spatially correlated porosity and log(permeability) sequences from north-central North Sea Brae oilfield

well core, Geophysical Journal International 148, 426-442.

Leary, PC (2002) Fractures and physical heterogeneity in crustal rock, in Heterogeneity of the Crust and Upper Mantle – Nature, Scaling and Seismic Properties, J. A. Goff, & K. Holliger (eds.), Kluwer Academic/Plenum Publishers, NewYork, 155-186.

Leary, P.: Fractures and Physical Heterogeneity in Crustal Rock, In: J.A. Goff & K. Holliger (eds.) *Heterogeneity of the Crust and Upper Mantle – Nature, Scaling and Seismic Properties,* Kluwer Academic/Plenum Publishers, New York, 155-186 (2002).

Leary P.C. & L.A. Walter (2008) Crosswell seismic applications to highly heterogeneous tight gas reservoirs, First Break v.26, 33-39.

Leary P, Pogacnik J & Malin P (2012) Fractures ~ Porosity → Connectivity ~ Permeability → EGS Flow Stimulation, Proceedings Geothermal Resources Council 36th Annual Conference, Reno NV, 30 September – 3 October 2 2012.

Leary P, Malin P, Pogacnik J, Rugis J, Valles B, Geiser P, Lacazette A & Vermilye J (2013a) The GeoCritical Reservoir: Observing and Modeling Lognormal Permeability Structures in Crustal Fluid Flow, Bull. American Society of Petroleum Geologists (in press).

Leary PC, Malin PE, Ryan GA, Lorenzo C & Flores M (2013b) Lognormally distributed K/Th/U concentrations – Evidence for geocritical fracture flow, Los Azufres geothermal field, MX, Proceedings Geothermal Resources Council 36th Annual Conference, 29 Sep – 3 Oct, Las Vegas NV.

Leary P, Malin P, Pogacnik J, Geiser P, Lacazette A & Vermilye J (2013c) Shale Bodies as a GeoCritical Reservoir – Observing/Modeling Lognormal Permeability Structures in Shale Production, AAPG/SEPM/PETROCHINA/CUP Joint Research Symposium "Fine-grained sedimentary systems and unconventional resources", Sept 23-28 Beijing.

Lie, K.-A., Nilsen, H. M., Rasmussen, A. F. and Raynaud, X.: An unconditionally stable splitting method using reordering for simulating polymer injection. *Proceedings of ECMOR XIII*, Biarritz, France. (2012).

Lie, K.-A., Nilsen, H. M., Rasmussen, A. F. and Raynaud, X.: Fast simulation of polymer injection in heavy-oil reservoirs based on topological sorting and sequential splitting. 2*013 SPE Reservoir Simulation Symposium*, The Woodlands, Texas, USA. (2013).

Limpert E., W. Stahel & M. Abbt, 2001. Log-normal Distributions across the Sciences: Keys and Clues, BioScience, v.51, no. 5, 341–352.

Mannington, W. I., O'Sullivan, M. J., Bullivant, D. P. and Clotworthy, A. W. (2004). Reinjection at Wairakei-Tauhara: a modelling case study, 29th Workshop Geothermal Reservoir Engineering, Stanford University, Stanford, CA.

Marsan D., and C. J. Bean, 1999, Geophys. Res. Lett., 26, 275-278.

Marsan, D. and Bean, C.J. (1999). Multiscaling nature of sonic velocities and lithology in the upper crystalline crust: Evidence from the KTB main borehole. Geophysical Research Letters 26.

MWD, 1977, Broadlands Geothermal Field Investigation Report, Ministry of Works and Development, Wellington, New Zealand, June 1977.

O'Sullivan, M.J., Yeh, A. and Mannington, W.I. (2009). A history of numerical modeling of the Wairakei geothermal field, Geothermics 38, 155-168.

O'Sullivan, MJ (2010) Geothermal fluid dynamics, 17th Australasian Fluid Dynamics Conference, Auckland NZ, 5-9 Dec.

Ponting D. K., Corner point geometry in reservoir simulation, King P. R., Ed., *The Mathematics of Oil Recovery*, p. 45–65, Oxford University Press, Oxford. (1992).

Ricard, L. P., M. G. Trefry, L. B. Reid, S. Corbel, L. Esteban, J.-B. Chanu, P. G. Wilkes, G. B. Douglas, A. H. Kaksonen, D. R. Lester, G. P. Metcalfe, L. Pimienta, S. Gutbrodt, S. Tressler, G. Bloomfield, C. Evans and K. Regenauer-Lieb, Report 5, Project 4: Productivity and Sustainability of Low-Temperature Geothermal Resources, CSIRO Earth Science and Resource Engineering, Australian Resources Research Centre, ISBN 978-0-643-10909-4.

Rugis, J., Leary, P., Alvarez, M., Malin, P.: *Towards crustal reservoir flow structure modelling through interactive 3D visualisation of MEQ & MT field data*. Proc. 33rd New Zealand Geothermal Workshop, Auckland, New Zealand. (2011).

Shiomi, K., Sato, H., and Ohtake, M., 1997, Broadband power-law spectra of well-log data in Japan, Geophys. J. Int. 130:57-64.

Smith L & Freeze RA, 1979, Stochastic analysis of steady state groundwater flow in an unbounded domain, 2. Two-dimensional simulation, Water Resources Research 15, 1543-1559.

Theis, CV, 1935, Transactions of the American Geophysical Union, Part 2, 519-524, August 1935.

Theis, CV, 1952, The relation between lowering of the piezometric surface and the rate and duration of discharge of a well using ground water storage, Ground Water Notes No 5, Hydraulics, United States Geological Survey, Water Resources Division, Ground Water Branch.

US Energy Information Administration (2011) Distribution and Production of Oil and Gas Wells by State, www.eia.gov/pub/oil_gas/petrosystem/all-years-states.xls.

Warren JE & Skiba FF, 1964, Macroscopic dispersion, Society of Petroleum Engineers Journal, SPE648, 215-230.

White, P. J., Lawless, J. V., Terzaghi, S. and Okada, W. (2005). Advances in subsidence modelling of exploited geothermal fields, Proceedings World Geothermal Congress 2005.

Wood, C.P. (1992): Geology of the Rotorua geothermal system. Geothermics, 21: 25-41.

Yeh, A. & O'Sullivan, M.J., 2007, Computer modelling subsidence in geothermal fields, Proc. 29th NZ Geothermal Workshop, University of Auckland, 9p.

APPENDIX A – RESERVOIR WELL-LOG SPECTRAL SYSTEMATICS

Figs A1-A3 illustrate features of *in situ* spatial fluctuations recorded by well logs run in wellbores in reservoirs worldwide (Leary 2002). Fig A1 (left) is a numerical well-log in which a sequence of zero values is followed by a step-change to unit values. The Fourier transform coefficients of a step function are known to scale inversely with wavenumber, hence the power-spectrum scales inversely as the wavenumber squared (Bracewell 1978). Fig A1 (right) shows the Fourier power-spectrum of Fig A1 (left), plotted as a straight line (blue) on log-log axes; the numerical fit to the spectrum (red) gives spectral slope -1.983 ~ -2.

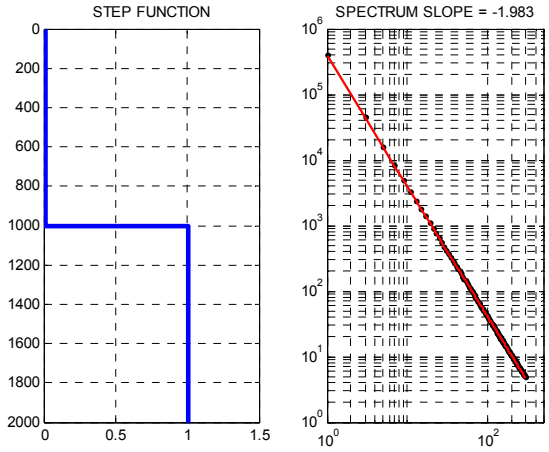

Figure A1 A simple step function in a material property with depth (e.g. % and meters) and its spatial spectrum (relative power and fluctuations per 1000 m). The slope is ~ -2.

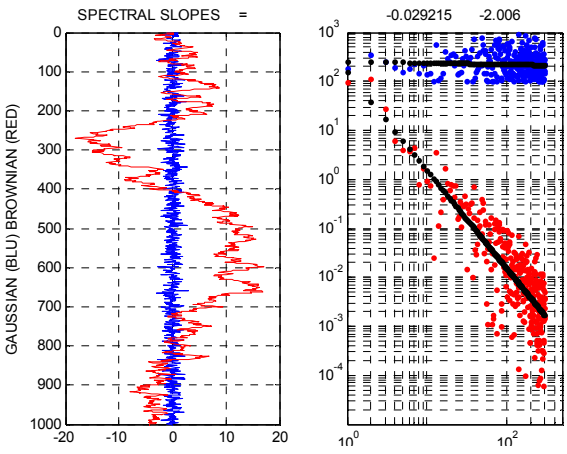

Figure A2. The same as Fig. A1, but for the cases in which the properties distributions are White (blue) and Brownian (red) noise. The respective spectra have slopes of 0 and -2.

Fig A2 (left) shows a 'white noise' sequence of uncorrelated (Gaussian) random numbers (blue) and its cumulative integral of correlated (Brownian) random numbers (red). Fig A2 (right) shows that the white noise power spectrum (blue) fluctuates around flat (zero slope) trend while the Brownian noise power-spectrum (red) fluctuates around trend of slope -2. Neither spectral slope is observed for reservoir well logs except when (i) poor data where only instrument white noise is observed; or (ii) where well-logs pass through major unconformities such as sediment/igneous contacts.

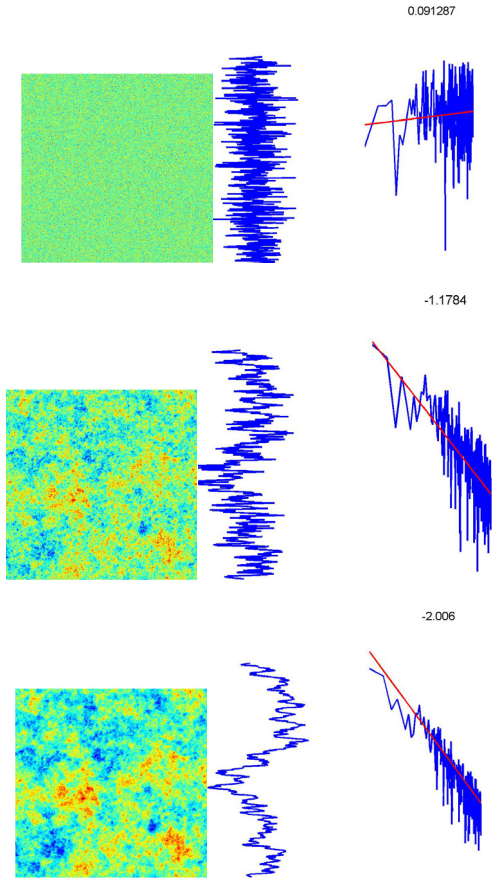

Figure A3 Map view comparisons of the 3 types of rock hetrogeneity discussed in this paper, along with their material property well logs and spectral contents.

Fig A3 (left) shows 2D spatial fluctuation arrays for 'white noise' (top), 'Brownian noise' (bottom) and the intermediate case '1/k noise' (center). Fig A3 (right) shows sample well-log 1D sequences across each of the noise arrays, with the associated power spectra. As in Figs A1-A2, the white noise and Brownian noise sequences have spectral trends of slope ~ 0 and ~ -2, respectively. The center array has a spectral power-law trend ~ -1. Visual inspection of field well-log fluctuation sequences indicates that *in situ* fluctuations resemble '1/k' noise sequences rather than white or Brownian noise sequences. We can therefore conclude that 2D and 3D array sequences of crustal property fluctuations resemble the spatial correlation seen in the center array rather than either the top or the bottom array. Visual inspection of the 2D arrays indicates that small-scale sampling of the white noise array gives a good estimate of the large-scale spatial behavior of the array, while extensive small-scale sampling of the Brownian noise array can indicate locally extensive spatial regions either well above or well below the overall mean; 2D Brownian noise thus resembles a noisy step-function

sequence as can occur in sedimentary sections. In contrast, small-scale spatial sampling of the '1/k noise' array achieves neither of these sampling goals at any scale length. These spatial fluctuation features are independent of scale. The only reliable information we have about 1/k and Brownian noise sequences are (i) the larger the spatial scale, the greater can be fluctuation amplitudes, and (ii) the location of the large amplitude fluctuations are unknowable from sparse small-scale sampling. It follows that the largest flow structure uncertainties occur at reservoir scales, and that the locations of these fluctuation extremes need to be observed rather than predicted (Leary et al 2013a).

APPENDIX B – RESERVOIR HETEROGENEITY WELL-CORE SYSTEMATICS

Figures B1-3 illustrate the well-core poroperm empirical relation (2) above, $\delta\varphi \sim \delta\log\kappa$, linking *in situ* porosity φ *to in situ* permeability κ in clastic reservoir rock (Leary & Al Kindy 2002; Leary & Walter 2008; Leary, Pogacnik & Malin 2012; Leary et al 2013b). As indicated by the lognormality expression (3) above, relation (2) can be restated as $\delta\kappa \sim \kappa\delta\varphi$. Warren & Skibas (1964) derive an equivalent relation in an attempt to explain the lognormality of well-core permeability first noted by Law (1944).

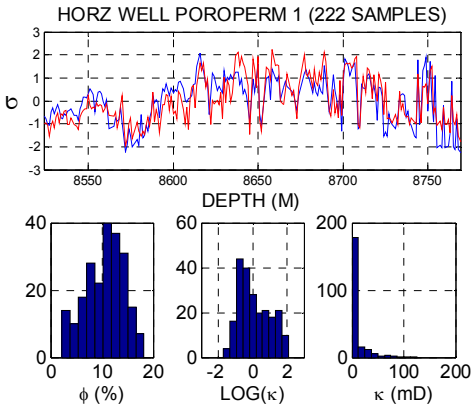

Figure B1 These plots compare the relative relations between lateral porosity and permeability distributions in highly hetrogenous rocks. The top plot compares normalized, unit variance porosity and log(permeability) as a function of well depth. The bottom plots show the distributions of porosity, log(permeability), and permeability. In both sets of plots it can be seen that the log(permeability is more close related to porosity than permeability itself.

The representative clastic reservoir well-core poroperm fluctuation sequences displayed in Figs 1-3 show a depth sequence of well-core porosity spatial fluctuations in blue overlayed by the spatial fluctations of log(permeability) in red. The fluctuation sequences are normalised to zero-mean/unit-variance format; that is, the fluctuation amplitudes are in units of trace standard deviation σ. The coefficient of spatial correlation is typically ~85%. Beneath each fluctuation plot are histrogram showing that typically porosity is normally distributed while permeability is lognornally distributed.

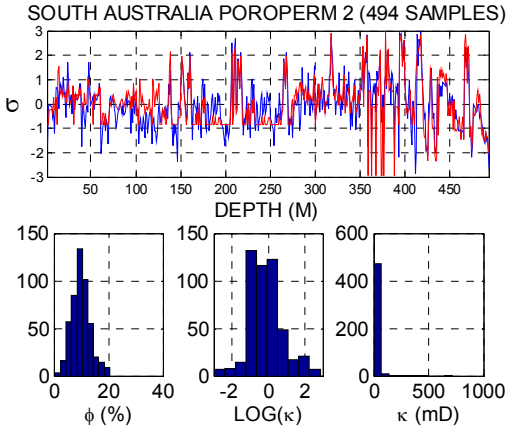

Figure B2 The same as in Figure B1.

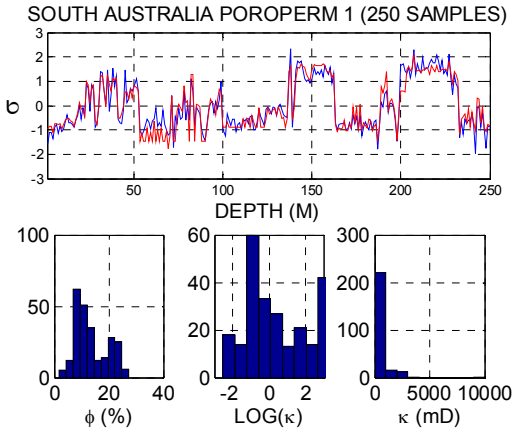

Figure B3 The same as in Figures B1 and B2.

Very few well-core poroperm data are available from geothermal fields. Fig B4 shows available data are consistent with the clastic reservoir data of Figs 1-3 (left-hand data from the Bulalo field, Philippines; right-hand data from the Ohaaki field, New Zealand; Leary et al 2013b).

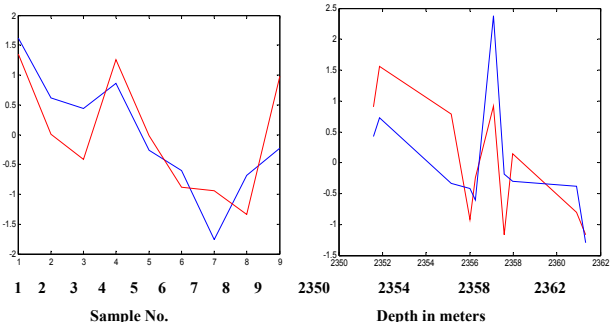

Figure B4 Normalized, unit variance porosity and log(permeability) data from Philippine and New Zealand geotheraml fields.